Table XVII. C_3H_4 Results for NEMO I, II, and III

	SCF	NEMO I	NEMO II	NEMO III[a]
$\frac{1}{2}\Sigma_i n_i\epsilon_i$	−39.10	−39.06	−38.95	−38.92
T	115.071	114.91	115.19	115.04
2e (HFMO)	−0.38	−0.36	−0.35	−0.39
1e	−0.59	−0.62	−0.58	−0.57
$7a_1$	−0.60	−0.63	−0.55	−0.60
$6a_1$	−0.70	−0.75	−9.71	−0.73
$5a_1$	−0.94	−0.92	−0.91	−1.00
Q(C1)	−0.226	−0.57		−0.206
Q(C2)	−0.037	+0.22		−0.058
Q(C3)	−0.406	−0.04		−0.342
Q(H4)	0.180	+0.21		0.143
Q(H5, 6, 7)	0.163	+0.06		0.154
Total energy	−115.597			−115.248
−E/T	1.0044			1.0019

			C_m's			
F_{ij}^{ZO}	SCF	NEMO	C 1s	C 2s	C 2p	CH
1C $2p_z$, 1C 2s	−0.186	−0.210	0.95	0.22	0.50	0.22
2C $2p_z$, 2C 2s	0.129	0.155	0.97	0.32	0.56	
3C $2p_z$, 3C 2s	0.056	0.034	0.98	0.42	0.62	0.26

[a] General method.

SCF density matrices and compare them with *ab initio* SCF results for C_2H_2, C_2H_6, and C_2H_4 in Table XVI. We find that α's for H are given accurately, as are anisotropies for C 2p α's. Errors for CH_2 and CH_3 carbons are similar in this series of compounds. NEMO III eigenvalues and orbital populations for C_3H_4 are compared with SCF results and with NEMO I and II results in Table XVII. The zero-overlap algorithm gives reasonable results for all four compounds. We also wish to perform calculations in which the ligands of the metal atom are H_2O and NH_3, and have therefore calculated NEMO III α's for H_2O and NH_3. The results (Table XVI) are similar to those for hydrocarbons.

Appendix D

The derivation of energy differences for transitions of filled and half-filled b_{1g} is as follows:

$$E(^2B_{1g}) = 2H_i + H(b_{1g}) + J_{ii} + 2J(i, b_{1g}) - K(i, b_{1g})$$

$$E(^2i) = H_i + 2H(b_{1g}) + J(b_{1g}, b_{1b}) + 2J(i, b_{1b}) - K(i, b_{1g})$$

$$\Delta E = H(b_{1g}) - H_i + J(b_{1b}, b_{1b}) - J_{ii}$$

$$\epsilon_{b_{1g}}{}^{\alpha} = H(b_{1g}) + 2J(i, b_{1g}) - K(i, b_{1g})$$

$$\epsilon_i{}^{av} = H_i + J_{ii} + J(i, b_{1g}) - 0.5K(i, b_{1g})$$

$$\Delta\epsilon = H(b_{1g}) = H_i - J_{ii} + J(i, b_{1g}) - 0.5K(i, b_{1g})$$

$$E = \Delta\epsilon + J(b_{1g}, b_{1g}) - J(i, b_{1g}) + 0.5K(i, b_{1g})$$

Arrhenius Preexponential Factors for Primary Hydrogen Kinetic Isotope Effects[1]

Mary E. Schneider and Marvin J. Stern*

Contribution from the Belfer Graduate School of Science, Yeshiva University, New York, New York 10033. *Received June 30, 1971*

Abstract: "Exact" model-reaction calculations are used to determine the lower limit to the Arrhenius preexponential factors, A_Q, for primary deuterium kinetic isotope effects in the harmonic approximation and in the absence of quantum mechanical tunneling. Attempts are made to force the A_Q values as low as possible solely through adjustments in the force constant changes, at the isotopic positions, between reactants and transition states. Values of A_Q lower than ~0.7 could not be achieved without making the models so mechanistically unreasonable as to render the results meaningless. A more conservative estimate of the lower limit, *viz.*, $A_Q \gtrsim 0.5$, is obtained by considering the lowest value found for the Arrhenius preexponential factor of the purely quantum mechanical contribution to a kinetic isotope effect to be the lower limit to the preexponential factor of the entire isotope effect. This conclusion is in excellent agreement with a prediction made by Bell on the basis of a less rigorous theoretical treatment and lends support to the common practice of interpreting experimental values of A_Q significantly lower than 0.5 as due to the operation of tunneling in the reactions.

The Arrhenius preexponential factors A_Q for primary hydrogen isotope effects, according to the equation

$$\ln (k_H/k_D) = \ln A_Q + B/T \qquad (1)$$

have been used for the detection of quantum mechanical tunneling in reactions involving, primarily, proton or hydrogen-atom transfer.[2] Bell, using a very simple model for a hydrogen-transfer reaction, predicted that values of A_Q should, in the absence of tunneling, be restricted to the range $0.5 \leq A_Q \leq 2^{1/2}$ and usually close to 1.0.[3] Experimental values[4] of A_Q significantly lower than 0.5 for primary hydrogen kinetic isotope effects have been interpreted as due to the operation of quantum mechanical tunneling in the reactions.[2]

(1) Supported in part by the U. S. Atomic Energy Commission under Contract AT(30-1)-3663.

(2) See the review by E. F. Caldin, *Chem. Rev.*, **69**, 135 (1969).

(3) R. P. Bell, "The Proton in Chemistry," Cornell University Press, Ithaca, N. Y., 1959, Chapter XI.

(4) Most reported experimental values of A_Q were determined by taking the ratio of the individual Arrhenius preexponential factors for the protium and deuterium reactions, $A_Q = A_H/A_D$, whereas in this work we determine A_Q directly according to eq 1. If the data fit the Arrhenius equation exactly, the two methods yield identical results. However, for the room temperature region, even computer-generated kinetic isotope effect data are not fit exactly by eq 1. We have compared the two methods, using actual experimental data for several reactions, and have found differences in the resulting corresponding A_Q values of less than 0.05 unit.

Table I. Force Constants for Starting and "Lowest Intercept" Models[a-c]

Simple Acid Ionization Reaction

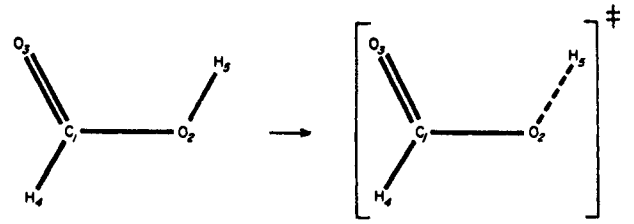

O···H str = [7.2, −3.6, −5.4]; $CO_{(2)}$ str-O···H str int'n = [0.42, 0.21, 0.00]; CO···H bend = [0.75, 0.37, 0.19]; O···H str-CO···H bend int'n = [0.21, 0.11, 0.00]; $CO_{(2)}$ str-CO···H bend int'n = [0.26, 0.13, 0.39]; HCO···H tors = OCO···H tors = HCO···H tors-OCO···H tors int'n = [0.034, 0.017, 0.0001]; HCOO oop-HCO···H tors int'n = HCOO oop-OCO···H tors int'n = [0.0082, 0.0041, 0.0001]

Hydrated Acid Ionization Reaction[e]

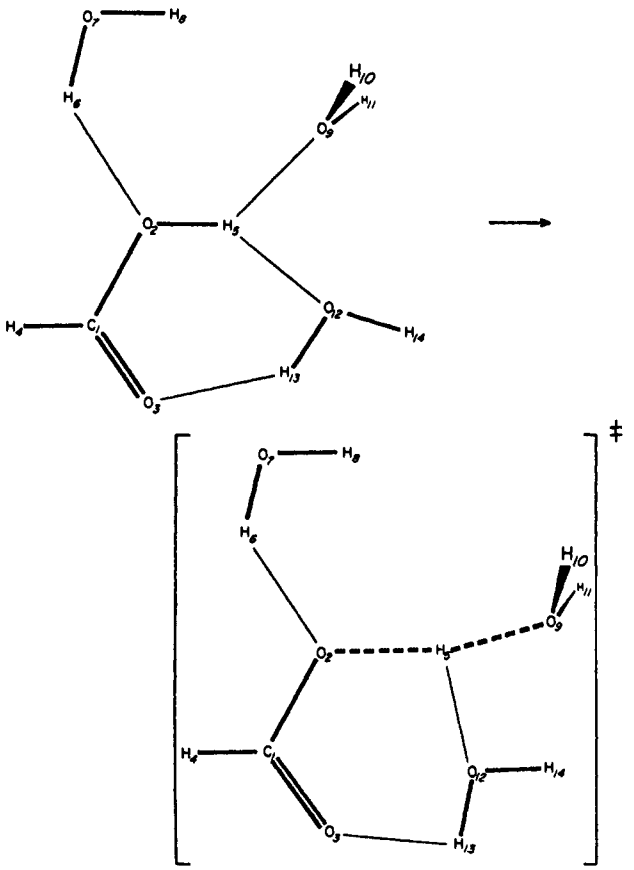

$O_{(2)}$···H str = [7.25, 0.72, 0.25]; $O_{(9)}$···H str = [0.14, 0.72, 0.25]; $OH_{(5)}$ str = [0.14, 0.22, 0.01]; $O_{(2)}$···H str-$O_{(9)}$···H str int'n = [dna, 3.1, 2.7]; $CO_{(2)}$ str-$O_{(2)}$···H str int'n = [0.42, 0.21, 0.005]; O···H···O bend = [0.0139, 0.0069, 0.0030]; CO···H bend = [0.75, 0.37, 0.19]; $HO_{(2)}$···H bend = [0.0069, 0.0104, 0.0050]; $HO_{(9)}$···H bend = [0.014, 0.070, 0.005]; $HOH_{(5)}$ bend = [0.014, 0.021, 0.005]; OH···$O_{(2)}$ bend = [0.0139, 0.0052, 0.0030]; OH···$O_{(9)}$ bend = [0.0035, 0.0052, 0.0030]; $O_{(2)}$···H str-CO···H bend int'n = [0.21, 0.11, 0.30]; $CO_{(2)}$ str-CO···H bend int'n = [0.26, 0.13, 0.39]; $CO_{(2)}$HH oop = [0.0044, 0.0067, 0.0030]; $H_{(5)}O_{(12)}$HH oop = [0.0089, 0.0135, 0.0050]; $O_{(2)}$···$H_{(5)}$OO oop = [0.0089, 0.0135, 0.0060]; HCO···H tors = OCO···H tors = HCO···H tors-OCO···H tors int'n = [0.034, 0.017, 0.005]; $O_{(2)}$···H···OH tors = [0.0007, 0.0030, 0.0003]; $O_{(2)}$···$HOH_{(13)}$ tors = [0.0050, 0.0005, 0.0005[f]]; CO···$HO_{(12)}$ tors = [0.0007, 0.0005, 0.0005[f]]; $O_{(3)}HOH_{(5)}$ tors = [0.0050, 0.0030, 0.0010]; HCOO oop-HCO···H tors int'n = HCOO oop-OCO···H tors int'n = [0.0082, 0.0041, 0.0100]

Radical-Abstraction Reaction

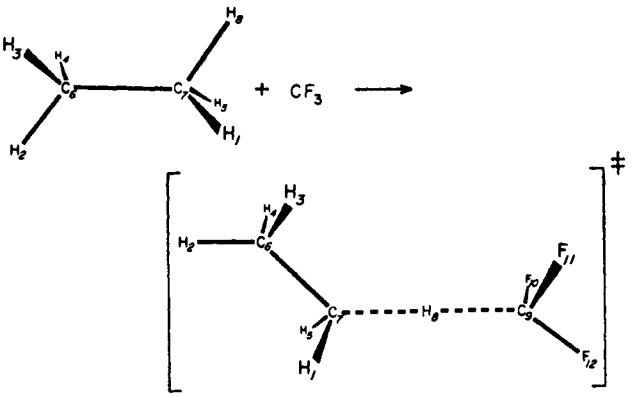

$C_{(7)}$···H str = [5.00, 0.53, 0.0001]; $C_{(9)}$···H str = [dna, 0.53, 5.00]; $C_{(7)}$···H str-$C_{(9)}$···H str int'n = [dna, 1.7, 3.5]; FC···H bend = [dna, 0.41, 0.21]; C···H···C bend = [dna, 0.10, 0.05]; CC···H bend = [0.68, 0.34, 0.17]; HC···H bend = [0.52, 0.26, 0.13]; $HCCH_{trans}$ tors = $H_{(2)}$CC···H tors = [0.0033, 0.0033, 0.0033[d]]

β-Elimination Reaction[g]

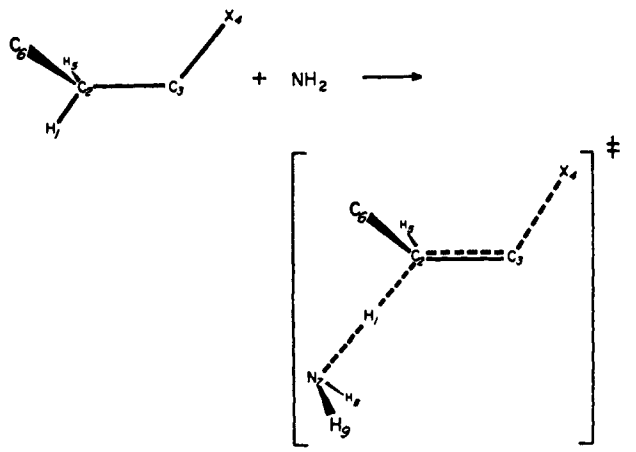

C···H str = [4.5, 2.3, 3.5]; N···H str = [dna, 3.3, 1.0]; C···X str = [4.0, 2.0, 1.0]; C···C str = [4.4, 7.0, 4.0]; C···H str-C···C str int'n = [dna, 3.4, 5.5]; N···H str-C···C str int'n = [dna, −1.6, −3.0]; C···X str-C···C str int'n = [dna, 3.0, 5.0]; HC···H bend = [0.53, 0.27, 0.14]; HN···H bend = [dna, 0.47, 0.20]; C···H···N bend = [dna, 0.105, 0.075]; C···C···H bend = CC···H bend = [0.68, 0.34, 0.17]; $H_{(8)}$NC···C tors[h] = NC···C···X tors[h] = [dna, 0.010, 0.003]

Decarboxylation Reaction

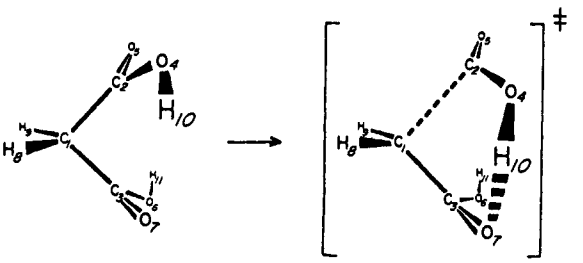

O···H str = [dna, 0.20, 0.05]; $O_{(4)}$H str = [7.7, 4.0, 2.0]; C···C str = [4.40, 0.20, 0.05]; $CO_{(4)}$ str = [5.0, 6.0, 3.0]; $CO_{(7)}$ str = [12.1, 11.1, 5.0]; O···H str-C···C str int'n = [dna, 0.80, 0.65]; CO···H bend = [dna, 0.050, 0.010]; $CO_{(4)}$H bend = [1.00, 0.55, 0.25]; CC···C bend = [1.1, 1.1, 0.5]; HC···C bend = [0.68, 0.62, 0.17]; C···$CO_{(4)}$ bend = C···$CO_{(5)}$ bend = [1.00, 0.90, 1.25]; $OC_{(2)}O$ bend = [1.00, 0.75, 1.25]; C···COO oop = CCOO oop = OCCO oop[i] = [0.20, 0.20, 0.20[d]]; C···COH tors = CCOH tors = $H_{(9)}$C···$CO_{(5)}$ tors = $H_{(8)}CCO_{(7)}$ tors = [0.100, 0.100, 0.050]

Table I (*Continued*)

[a] In the transition-state drawings dashed lines are used for breaking or forming bonds directly involved in the reaction coordinates ("reacting bonds"). The deuterium substitutions were always made at the primary hydrogen positions (*i.e.*, the positions involved in reacting bonds). The slanted atom numbers are used for identification in the force constant specifications. [b] The complete reactant and starting transition-state force fields and geometries have been listed by Schneider.[19] Only those force constants that were adjusted are given here (in rounded-off form). Three values are given for each force constant; they are, in order, reactant value, starting transition-state value, lowest intercept transition-state value. Force constants that do not appear in the reactant force field are designated dna; their effective reactant value is zero. Each force constant applies to all internal coordinates that fit the description given. Atom numbers (appearing as parenthesized subscripts) are used for specificity when only selected internal coordinates are referenced. Atom numbers are sometimes used redundantly to avoid possible misinterpretation. In the internal coordinate descriptions a reacting bond is *always* indicated by three dots, except when it forms part of the *plane* of an out-of-plane wagging coordinate. The following abbreviations are used to designate internal coordinates: str = change in bond length; bend = change in angle between two adjacent bonds (second atom is the vertex); tors = torsional motion (second and third atoms define the axis); oop = out-of-plane wagging motion (last three atoms define the plane). More detailed descriptions of the internal coordinates are available.[19] The abbreviation int'n refers to the interaction between two internal coordinates. The units of the force constants are: str and str–str int'n, mdyn/Å; bend, tors, oop, and interactions among these, mdyn Å/rad^2; str–bend int'n, mdyn/rad. [c] Force constants with common values in reactant, starting transition state, and lowest intercept transition state were not necessarily varied together as a group. Only force constants for equivalent, or very nearly equivalent, internal coordinates were varied in groups. [d] Increasing or decreasing this force constant, from the starting transition-state value, increased A_Q. [e] The thin lines in the drawings indicate hydrogen bonds. [f] Increasing this force constant, from the starting transition-state value, increased A_Q. The effect of further decreasing this already very small force constant was not investigated. [g] Cutoff model; see footnote 17. [h] The $N_{(7)}$–$C_{(2)}$ linear connection is treated as an ordinary bond in the torsion coordinate. [i] Note that this designation refers to the four OCCO oop coordinates involving either $O_{(4)}$ and $O_{(5)}$ or $O_{(6)}$ and $O_{(7)}$.

Within the Born–Oppenheimer approximation the potential energy surfaces and, consequently, the mechanisms of isotopic reactions are identical. However, the extent of tunneling is greater for protium than for deuterium so that there should be more positive curvature at the low-temperature end of an Arrhenius plot for the protium reaction than for the corresponding deuterium reaction. As a result, $A_Q = A_H/A_D$[4] should be lower than it would be in the absence of tunneling. Values of A_Q as low as 0.04 ± 0.01[5] and 0.15[6] have been reported.

Bell's model is a reactant in which the hydrogen atom of interest is bonded to a very heavy rigid group, X, and a transition state in which the XH-stretching force constant is zero and the force constants for two bending motions of the hydrogen atom, assumed to be orthogonal to each other and to the stretching motion, are altered from the reactant. The model is not what one would now call an "exact" model for an isotope effect calculation.[7] Because of the assumed orthogonality of the stretching and bending motions, the three isotope-dependent frequencies are shifted, upon deuterium substitution, by factors of exactly $2^{-1/2}$. Bigeleisen has pointed out that, according to the Teller–Redlich product rule, such an isotopic shift pattern cannot be achieved by real molecules.[12]

An identical model was used by Swain, *et al.*, in deriving a relationship between tritium and deuterium kinetic isotope effects in the absence of tunneling.[13] It has been shown,[14] using "exact" model calculations, that this relationship is not valid for many common reaction conditions, although for sizable magnitude, normal direction ($k_{light} > k_{heavy}$), *primary* hydrogen isotope effects, the relationship is reasonably accurate.

The present work is an "exact" model-calculation evaluation of Bell's prediction that, in the absence of tunneling, the Arrhenius A_Q factors must be ≥ 0.5. The model systems are restricted to those corresponding to primary hydrogen kinetic isotope effects of sufficiently large magnitudes to be characterized by regular temperature dependences.[15,16] Such effects would be the most likely ones to be involved in an experimental study of tunneling.

Model Systems and Calculations

The underlying purpose of our calculations was to determine the lower limit to A_Q in the absence of tunneling. In particular, we addressed ourselves to the question of whether or not it is possible to force A_Q below 0.5 by judicious, but arbitrary, adjustments of transition-state force constants.

Our calculations were carried out with five basic model types which we feel are representative of a sizable fraction of all possible types of reactions in which one would observe primary hydrogen kinetic isotope effects. These models include both small and large molecules, both simple and complex reaction coordinates, and both normal and inverse isotope effects. The basic models are (i) abstraction of hydrogen from ethane by trifluoromethyl radical; (ii) formic acid ionization; (iii) solvent-assisted ionization of hydrated formic acid; (iv) bimolecular β-hydrogen elimination from

(5) R. P. Bell, J. A. Fendley, and J. R. Hulett, *Proc. Roy. Soc., Ser. A*, **235**, 453 (1956).

(6) E. S. Lewis and L. H. Funderburk, *J. Amer. Chem. Soc.*, **89**, 2322 (1967).

(7) We define an "exact" model calculation as one which corresponds to Bigeleisen's statistical-thermodynamic, transition-state treatment of kinetic isotope effects,[8,9] in the harmonic approximation, ignoring condensation effects and quantized rotational degrees of freedom. Bigeleisen's "exact" equation can be abbreviated as[10]

$$k_H/k_D = (\nu_{HL}^{\ddagger}/\nu_{DL}^{\ddagger})(VP)(EXC)(ZPE)$$

where k_H/k_D is the ratio of isotopic rate constants, $\nu_{HL}^{\ddagger}/\nu_{DL}^{\ddagger}$ is the isotopic ratio of zero or imaginary frequencies representing motion along the reaction coordinate of the transition state, *VP* is a vibrational frequency product term, *EXC* is a vibrational excitation term, and *ZPE* is a zero point energy term. In order to qualify as "exact," a model reaction must be self-consistent and obey all the relationships inherent in the derivation of the above equation. Adherence to these criteria is assured by calculating the harmonic vibrational frequencies of the isotopic reactants and transition states using isotope-independent geometries and force fields. The programs used for these calculations have been described previously.[10,11]

(8) J. Bigeleisen, *J. Chem. Phys.*, **17**, 675 (1949).

(9) J. Bigeleisen and M. Wolfsberg, *Advan. Chem. Phys.*, **1**, 15 (1958).

(10) M. Wolfsberg and M. J. Stern, *Pure Appl. Chem.*, 8, 225 (1964).

(11) J. H. Schachtschneider and R. G. Snyder, *Spectrochim. Acta*, **19**, 117 (1963).

(12) J. Bigeleisen, "Tritium in the Physical and Biological Sciences," Vol. I, International Atomic Energy Agency, Vienna, 1962, p 161.

(13) C. G. Swain, E. C. Stivers, J. F. Reuwer, Jr., and L. J. Schaad, *J. Amer. Chem. Soc.*, **80**, 5885 (1958).

(14) M. J. Stern and P. C. Vogel, *ibid.*, **93**, 4664 (1971).

(15) P. C. Vogel and M. J. Stern, *J. Chem. Phys.*, **54**, 779 (1971).

(16) M. J. Stern, M. E. Schneider, and P. C. Vogel, *ibid.*, **55**, 4286 (1971).

modified ("cutoff"[17]) alkyl-X with amide ion (X is an "atom" with mass 80 amu, representative of halogen or any heavy group[18]); (v) decarboxylation of malonic acid. The reactions corresponding to these models are depicted in Table I. In general, the models were constructed so as to represent reactions with potential barriers of intermediate curvature. The details of the starting basic models (geometries and force fields) are available;[19] only the primary motions of the transition-state reaction coordinates are described below.

In the radical-abstraction model the reaction coordinate corresponds to the simultaneous rupture of one C···H bond and formation of the other. In the simple acid ionization model the reaction coordinate corresponds to unconcerted rupture of the O···H bond. The reaction coordinate in the solvent-assisted acid ionization model corresponds to simultaneous rupture of the acidic O···H bond and transformation, from hydrogen bond to covalent bond, of the O···H bond to one of the solvating water molecules. In the β-elimination model the reaction coordinate corresponds to rupture of the C···H and C···X bonds and formation of the N···H bond and C···C double bond, all occurring simultaneously. The reaction coordinate of the cyclic transition state in the decarboxylation model corresponds to simultaneous rupture of the C···C bond and formation of the O···H bond.

Our general procedure was to start with the above-mentioned force fields and systematically vary individual transition-state force constants (or small groups of force constants for equivalent or very nearly equivalent internal coordinates) in such a manner as to drive the corresponding Arrhenius intercepts, ln A_Q, as low as possible for each type of force constant change. The intercepts were each obtained by least-squares fitting to eq 1 of four "exact" isotope effect values over the temperature range 300–375°K. The force constant adjustments for each stretch, bend, torsion, out-of-plane wag, and internal coordinate interaction that individually produced the lowest A_Q factors were combined to form a force field that should correspond to nearly the lower limit to A_Q (at 300–375°K) for the particular model type under consideration.[20] The final models obtained by the procedure outlined above are referred to in this report as "lowest intercept" models.

In varying individual transition-state force constants in the search for lowest A_Q factors, we allowed ourselves fairly wide latitudes. In general, transition-state force constants were allowed to vary from several times, to a small fraction of, their corresponding reactant, or other stable molecule, values. The individual force constant changes, between reactants and lowest intercept transition states, were restrained within the *general* bounds of such changes assumed to be operative, for specific *types* of force constants, in real reactions. However, the individual force constant changes were combined into the lowest intercept models, without much regard for mechanistic credibility with respect to the particular model-reaction type under consideration.[21]

In addition to the A_Q analysis discussed above, calculations on the purely quantum mechanical contributions to the kinetic isotope effects were carried out. Since

$$\ln [(k_H/k_D)(\nu_{HL}^{\ddagger}/\nu_{DL}^{\ddagger})^{-1}] = \ln A_f + B/T \quad (2)$$

is the equation, corresponding to eq 1, for the quantum mechanical kinetic isotope effect, A_Q and A_f are related by

$$\ln A_Q = \ln A_f + \ln (\nu_{HL}^{\ddagger}/\nu_{DL}^{\ddagger}) \quad (3)$$

As the purely classical contribution to an intermolecular isotope effect [ln $(\nu_{HL}^{\ddagger}/\nu_{DL}^{\ddagger})$] is always positive,[9] A_Q is always greater than A_f so that a lower limit to A_f is surely a lower limit to A_Q. Thus, for each A_Q value obtained, a corresponding A_f value was calculated with eq 3. (Such A_f values are, of course, identical with those that would have been obtained had the data been fit by least squares to eq 2 rather than to eq 1.)

Because of the possibility of a kinetic isotope effect temperature-dependence irregularity ("anomaly"),[15,16] we considered it necessary to establish that the particular value obtained for an A_Q factor was not the result of a fortuitous extrapolation from an anomalous region of the temperature-dependence curve. In such a case the intercept might be meaningless for the purposes of a tunneling study. Therefore, each model calculation was checked for temperature-dependence irregularities by calculating and plotting the isotope effect over the extended temperature range 20–2000°K. In only two instances did we observe such irregularities. In both cases they appeared in calculations for a β-elimination model when individual bending force constants (HN···H and C···H···N bends; see Table I) were adjusted (decreased) to such an extent that the magnitude of the isotope effect became very low [ln $(k_H/k_D) \approx -0.1$ at 300°K]. The irregularities appeared, in plots of ln (k_H/k_D) *vs.* log T, as very minor, high-temperature, inflection regions which most probably would have been "washed out" in the combined force field. Nevertheless, in order to be completely safe, we stopped adjusting at the point the inflection appeared, backtracked a little, and included in the final lowest intercept force field only force constant variations which *individually* produced completely regular temperature dependences.

Finally, we determined the sensitivity of the derived Arrhenius preexponential factors to the temperature range of the data considered. For each of the lowest

(17) The starting β-elimination reaction model was obtained by applying the "cutoff" procedure[18] to the model for β elimination from 2-butyl-X used in a study of the temperature dependences of kinetic isotope effects.[15] In order to reduce the size of the cutoff model "molecules" still further, the rules[18] for "proper" cutoff were not adhered to strictly with respect to one torsion coordinate. This deviation has no significance with respect to the present study. In addition, it had only very slight effect on the results of the calculations [<1.5% difference in ln (k_H/k_D) at 300°K].

(18) M. J. Stern and M. Wolfsberg, *J. Chem. Phys.*, **45**, 4105 (1966).

(19) M. E. Schneider, Ph.D. Thesis, Yeshiva University, New York, N. Y., 1971.

(20) Attempts were sometimes made to force the A_Q value of a combination model still lower by making additional changes in the model. Also, calculations were carried out in which individual force constant adjustments (from the starting models), which were not necessarily those individually producing the lowest A_Q values, were combined in several different ways. The results of these trial calculations always indicated that the combination consisting of the force constant adjustments that individually produced the lowest A_Q values was the combination with the lowest final A_Q value.

(21) In order to prevent our final lowest intercept models from becoming too unreasonable, the specific restrictions imposed on the allowed individual transition-state force constants were varied among the basic model types as well as among the internal-coordinate types. An enumeration of these restrictions is available.[19]

Table II. Kinetic Isotope Effects for Starting and Lowest Intercept Models

Model reaction	k_H/k_D, 100°K Start[a]	k_H/k_D, 100°K Li[b]	k_H/k_D, 300°K Start	k_H/k_D, 300°K Li	k_H/k_D, 1000°K Start	k_H/k_D, 1000°K Li
Radical abstraction	143	530	5.90	8.44	1.85	1.87
Simple acid ionization	4287	9375	14.85	17.26	2.15	2.19
Hydrated acid ionization	1726	11201	12.19	19.29	2.14	2.25
β elimination[c]	0.41	3.28	0.77	1.49	0.96	1.11
Decarboxylation	23	262	2.81	5.96	1.33	1.59

[a] Starting (unadjusted) model. [b] Lowest intercept model. [c] All of the individual transition-state force constant adjustments, when applied to the starting force field, still resulted in low magnitude, inverse ($k_H/k_D < 1$), kinetic isotope effects. However, when all of the adjustments were combined in the final, lowest intercept, force field, the resulting isotope effect was of low magnitude in the normal direction ($k_H/k_D > 1$).

Table III. Arrhenius Preexponential Factors for Lowest Intercept Models

Model reaction	300–375°K A_Q	300–375°K A_t[a]	Lowest value in 20–1000°K range A_Q	Lowest value in 20–1000°K range A_t	Lowest value in 20–1000°K range Temp, °K	Highest[b] value in 20–1000°K range A_Q	Highest[b] value in 20–1000°K range A_t	Highest[b] value in 20–1000°K range Temp, °K
Radical abstraction	0.964 ± 3[c]	0.721 ± 2[c]	0.941 ± 1	0.703 ± 1	425–500	1.173 ± 1	0.877 ± 1	20–50
Simple acid ionization	0.781 ± 4	0.568 ± 3	0.730 ± 1	0.530 ± 1	150–225	1.001 ± 5	0.727 ± 4	850–1000
Hydrated acid ionization	0.787 ± 3	0.566 ± 2	0.771 ± 1	0.555 ± 1	225–300	0.998 ± 1	0.718 ± 1	30–60
β elimination	0.950 ± 1	0.880 ± 1	0.944 ± 1	0.874 ± 1	375–450	1.073 ± 1	0.994 ± 1	60–75
Decarboxylation	0.899 ± 1	0.807 ± 1	0.895 ± 1	0.804 ± 1	200–275	1.000 ± 1	0.898 ± 1	20–50

[a] The models to which these A_t values correspond were constructed to produce the lowest A_Q values. Occasionally, a different model produced a slightly lower A_t value; the differences were never larger than ~0.005 unit in A_t. [b] Note that the models were *not* constructed to produce the highest A_Q values. [c] The appended error limits are given as 10^3 times the estimated standard deviation (propagated from the estimated standard deviation of ln A_Q) or 1, whichever is greater.

intercept models, we carried out 36 additional least-squares fits to eq 1, each employing kinetic isotope effect values at four temperatures, in all covering the temperature range 20–1000°K. The temperature ranges of the individual sets of four temperatures overlapped considerably and varied in width from 15 to 30° at the low-temperature end to 150° at the high-temperature end.

Results and Discussion

The adjusted transition-state force constants for the final lowest intercept models are given in Table I. The corresponding reactant and starting (unadjusted) transition-state force constants are included for comparison. In each of the five cases the lowest intercept transition-state model was obtained from the starting transition-state model by a *net* lowering of force constants at the isotopic position. Because force constant changes involving only atomic positions removed from the site of isotopic substitution make only very small contributions to the overall isotope effect,[18,22] we usually adjusted only force constants for coordinates directly involving the primary hydrogen atom. In some cases, however, we also made adjustments in force constants for non-isotopic coordinates, especially when such adjustments might be expected to alter the nature of the reaction coordinate (*e.g.*, adjustments in force constants for internal coordinates involving reacting bonds). Generally, the values of the A_Q factors were about an order of magnitude less sensitive to variations in the force constants for these nonisotopic coordinates than for isotopic coordinates.

Table II lists the values of k_H/k_D at three temperatures for the starting and lowest intercept models. As expected[8–10] from the force constant differences between the starting and corresponding lowest intercept models, in each case k_H/k_D was higher for the latter.

The A_Q and A_t values obtained from the lowest intercept models are listed in Table III, and the A_Q temperature profiles for these models are shown in Figure 1. It is seen that the value of the Arrhenius preexponential factor is somewhat sensitive to the temperature region of the data considered but not so in an easily predictable manner.[23]

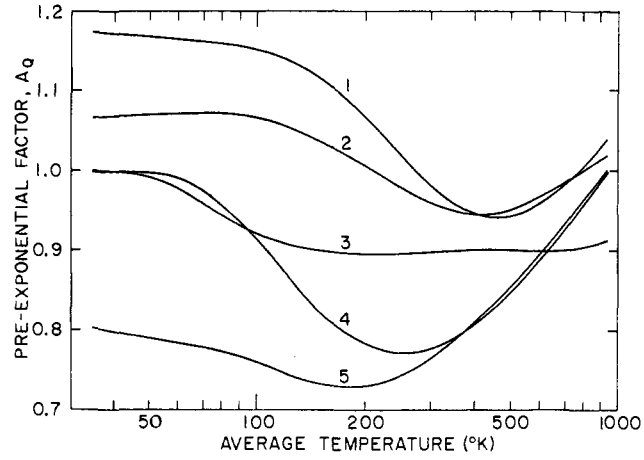

Figure 1. Dependence of Arrhenius preexponential factor, A_Q, on temperature range of data: curve 1, radical-abstraction reaction; curve 2, β-elimination reaction; curve 3, decarboxylation reaction; curve 4, hydrated acid ionization reaction; curve 5, simple acid ionization reaction.

(22) M. J. Stern and M. Wolfsberg, *J. Chem. Phys.*, **45**, 2618 (1966).

(23) At sufficiently low temperatures ln (k_H/k_D) approaches a true T^{-1} dependence so that A_Q becomes temperature independent. The value of the low-temperature limit to A_Q is independent of the force field and depends only on the molecular weights and moments of inertia of the isotopically substituted reactants and transition states.[10] At sufficiently high temperatures ln (k_H/k_D) can be described accurately by a first quantum correction, which has a T^{-2} dependence.[8,9] A T^{-2} dependence introduces positive curvature into a positively sloped, or negative curvature into a negatively sloped, ln (k_H/k_D) *vs.* T^{-1} plot. Thus, for a normal direction kinetic isotope effect, simple reasoning predicts that the intercept, ln A_Q, will increase monotonically with increasing temperature. However, "exact" model-calculation isotope effect values do not necessarily undergo a smooth transition from a T^{-1} to a T^{-2} temperature dependence, even when the temperature dependence is classified as regular.[15,24] In the curves shown in Figure 1 the expected monotonic

It is doubtful that additional force constant adjustments could be devised which would force the A_Q and A_f factors much below the values shown in Table III, without extending the models so far beyond what could be considered mechanistically reasonable as to make them meaningless. Our models, which were constructed not for mechanistic reasonableness, but specifically to produce low Arrhenius preexponential factors, did not result in values of A_Q less than ~0.7 nor values of A_f less than ~0.5.

Conclusions

There is probably no strictly defined lower limit to the value of the kinetic isotope effect Arrhenius preexponential factor, A_Q, that can result, in the harmonic approximation, solely from force constant changes, at the isotopic position, between reactant and transition state. The present study indicates that, for sizable magnitude primary hydrogen kinetic isotope effects, the *effective* lower limit to such A_Q values is ~0.7. A more conservative estimate, $A_Q \gtrsim 0.5$, is obtained by considering the lowest value found for the Arrhenius preexponential factor of the purely quantum mechanical contribution to a kinetic isotope effect (A_f) to be the lower limit to the preexponential factor of the entire isotope effect (A_Q). This conclusion is in excellent agreement with a prediction made by Bell on the basis of a less rigorous theoretical treatment[3] and lends support to the common practice of interpreting experimental values of A_Q significantly lower than 0.5 as due to the operation of quantum mechanical tunneling.

We wish to stress, however, that we have considered, and our conclusions are meant to apply to, only primary hydrogen kinetic isotope effects of sufficiently large magnitudes to be characterized by regular temperature dependences. We have estimated[16,25] that, in order for a pure primary or mixed primary–secondary hydrogen kinetic isotope effect to be assuredly associated with a regular temperature dependence, the value of k_H/k_D at 300°K must be greater than ~2.7 (regular at all temperatures) or less than ~0.5 (regular at least at room temperature and above).

increase in A_Q with increasing temperature does not occur until temperatures as high as ~200°K (for the simple acid ionization model) to ~650°K (for the decarboxylation model) are attained. We are indebted to Professor Jacob Bigeleisen for pointing out to us a significant error in our original analysis of the temperature variation of A_Q.

(24) M. J. Stern, W. Spindel, and E. U. Monse, *J. Chem. Phys.*, **48**, 2908 (1968).

(25) These estimates[16] were based, in part, on the results of the isotope effect temperature-dependence plotting procedure carried out in conjunction with the present investigation.

Electrogenerated Chemiluminescence. VIII. The Thianthrene–2,5-Diphenyl-1,3,4-oxadiazole System. A Mixed Energy-Sufficient System

Csaba P. Keszthelyi, Hiroyasu Tachikawa, and Allen J. Bard*

Contribution from the Department of Chemistry, The University of Texas at Austin, Austin, Texas 78712. *Received June 3, 1971*

Abstract: Electrogenerated chemiluminescence (ecl) resulting from reaction of the thianthrene (TH) cation radical and the 2,5-diphenyl-1,3,4-oxadiazole (PPD) anion radical in acetonitrile solutions is characterized by emission at wavelengths of both TH and PPD fluorescence. A consideration of the enthalpy of the reaction shows the process to be energy sufficient with respect to formation of excited singlet TH (430 nm) and to be energy deficient with respect to formation of excited singlet PPD (340 nm). The absence of a magnetic field effect on ecl emission at 430 nm also suggests the direct formation of singlet TH* on radical-ion annihilation. Emission at 340 nm probably arises from triplet–triplet annihilation of triplet PPD, formed either in the radical annihilation reaction or by energy transfer from triplet TH. Variations in the spectral distribution and the intensity of the ecl emission with the frequency of the applied potential steps were also investigated.

It has been convenient to classify reactions in electrogenerated chemiluminescence (ecl) as "energy sufficient" when the energy of the light produced is equal to or smaller than the enthalpy of the redox reaction for a single pair of reacting species producing ground-state molecules. For example, the reversible peak potentials for the oxidation (E_{p_a}) and reduction (E_{p_c}) of 9,10-diphenylanthracene (DPA) in *N*,*N*-dimethylformamide (DMF) solution (V *vs.* sce) are +1.35 and −1.89, respectively, and the energy of the first excited singlet (E_s) is 3.0 eV, so that, correcting for the difference between E_p and E^0 and estimating a small contribution for the entropy term, DPA ecl is an "energy-sufficient" system.[1] Ecl is also observed in mixed systems, that is, systems in which the electrogenerated oxidant and reductant are produced from different species. Typical examples of mixed-system chemiluminescence involve Wurster's Blue cation radical ($TMPD^{\cdot+}$) and chrysene anion radical,[2] $TMPD^{\cdot+}$ and $DPA^{\cdot-}$, and a number of other systems recently studied by Freed and Faulkner.[3] In all cases these were "energy-deficient" systems where the energy of

(1) L. R. Faulkner and A. J. Bard, *J. Amer. Chem. Soc.*, **91**, 209 (1969).

(2) A. Weller and K. Zachariassse, *J. Chem. Phys.*, **46**, 4984 (1967).

(3) D. J. Freed and L. R. Faulkner, *J. Amer. Chem. Soc.*, **93**, 2097 (1971).